*Massive Stars Across Redshifts in the Era of JWST and Large Surveys*
*Proceedings IAU Symposium No. 402, 2026*
*A. Wofford, N. St Louis, M. García, S. Simón-Díaz & L. M. Oskinova, eds.*
doi:10.1017/S1743921326106000

# Analyses of OB stars: abundances and stellar parameters

**N. Przybilla**

Universität Innsbruck, Institut für Astro- und Teilchenphysik, Technikerstr. 25/8, 6020 Innsbruck, Austria
email: norbert.przybilla@uibk.ac.at

**Abstract.** Model atmosphere analyses provide observational constraints that can be used to test models of OB stars to answer key questions of massive star research. In the focus are elemental abundances and atmospheric parameters, which in particular in the era of precise and accurate parallax measurements by the Gaia mission can be used to derive fundamental stellar parameters. An overview of the state-of-the-art of quantitative spectroscopy of OB stars is given, concentrating on one hand on the question of how well information can be extracted from observations, which is of particular interest on the eve of the upcoming large-scale spectroscopic surveys. On the other hand, existing observational results are confronted with model predictions, illuminating successes but also pointing out the open questions.

**Keywords.** stars: abundances, stars: atmospheres, stars: early-type, stars: evolution, stars: fundamental parameters, stars: massive

## 1. Introduction

Models for the structure and evolution of single massive OB-type stars that account for mass loss and rotation have recently reached a high degree of sophistication (e.g. Brott *et al.* 2011; Ekström *et al.* 2012; Chieffi & Limongi 2013; Choi *et al.* 2016). Although there is general agreement between the different codes with respect to evolution on the main sequence, the predictions of the models can differ significantly at later stages of evolution (e.g. Martins & Palacios 2013), so one can conclude that our understanding of massive star evolution still needs improvement. This is because all detailed assumptions (e.g. the treatment of convection), approximations (e.g., on the outer boundary condition or on chemical homogeneity on the ZAMS), and parameter choices (e.g., on values of diffusion coefficients) made initially influence the models when they are propagated in time. In the absence of experimental data or derivations from 3D hydrodynamic stellar evolution models, the only way to constrain these is by comparison of model predictions with observations – various stellar parameters and elemental abundances. That is, iteratively parameter sets are tested for their suitability to reproduce as many observational constraints as possible to choose the most appropriate ones, a process that can be refined whenever additional or improved observational constraints become available.

The situation got more complicated once it became clear that the vast majority of massive stars are part of binary (or higher) star systems and will interact with their companion stars during their lifetime (e.g. Chini *et al.* 2012; Sana *et al.* 2012), leading to matter accretion and spin up, or to stripping, to a common envelope phase, and to mergers. Due to the additional physics involved, the life cycles of stars in binary systems are drastically altered, complicating our understanding of their evolution (e.g. Marchant & Bodensteiner 2024). Further uncertainties for the evolution of massive stars come

© The Author(s), 2026. Published by Cambridge University Press on behalf of The International Astronomical Union.

https://doi.org/10.1017/S1743921326106000 Published online by Cambridge University Press

from magnetic fields. Strong organised surface magnetic fields are observed for ∼5–10% of massive stars (e.g. Grunhut *et al.* 2017; Schöller *et al.* 2017), but their presence has the potential to also drastically change predictions of evolutionary models of massive stars via mass-loss quenching, magnetic braking, and changes to angular momentum transport (Keszthelyi *et al.* 2022). Internally generated magnetic fields may be more widespread, but their exact role in massive star evolution still needs to be clarified.

## 2. Observational constraints on the evolution of massive stars: status quo

The simplest observational constraints on stellar evolution models are provided by counts of stars in different evolutionary phases, which can be performed in different galactic environments to trace the effects of initial chemical composition (metallicity) on the models. For the resolved stellar populations of the Local Group galaxies, one can determine, for example, the Wolf-Rayet (WR) to O-star ratio or the ratio of WC/WN subtypes of WR stars (see e.g. the discussion by Meynet & Maeder 2005), or the blue supergiant (BSG) to red supergiant (RSG) ratio $B/R$ (Eggenberger *et al.* 2002), which is very sensitive to mass loss, convection, and mixing processes (Langer & Maeder 1995; He *et al.* 2025). Alternatively, one can compare model predictions to observations of supernovae from different massive star progenitors, like the SN Ibc/SN II ratio (e.g. Georgy *et al.* 2009), covering a larger volume of the local cosmos. In all these cases, stellar evolution models for single stars that account for rotation provide improvements to explain the observations, but residual discrepancies remain.

Although the true rotational velocities of individual stars are difficult to determine (except for particular cases), the projected rotational velocity $v \sin i$ can be easily derived, independently of a full model atmosphere analysis. Recent examples are the rotational velocity distributions of hundreds of massive stars in the LMC from the VLT-FLAMES Tarantula Survey (Dufton *et al.* 2013) or from the IACOB survey of Galactic stars (de Burgos *et al.* 2024). Overall, a bi-modal distribution is found, which does not necessarily reflect the spin-rate of the stars at birth. Instead, the fast-rotating tail appears to stem from spin-up of the mass gainers in binaries, or from mergers, whereas the slow rotators are the results of efficient spin-down in the course of stellar evolution (de Mink *et al.* 2013).

Once model atmosphere analyses are involved for deriving stellar parameters, additional features in the Hertzsprung-Russell diagram (HRD) become accessible for comparison with model predictions. Of particular importance is the extent of the main sequence (MS), specifically of the terminal-age main sequence (TAMS). Using a volume-limited sample (<2.5 kpc) of about 700 massive stars, de Burgos *et al.* (2025) have presented the so far most ambitious investigation, locating the TAMS at ∼22.5 kK throughout the investigated luminosity range, partially in agreement and in disagreement with common stellar evolution models.

The necessity for stellar evolution models accounting for rotation was motivated by the presence of nuclear-processed matter already on the MS, in the form of nitrogen-rich stars. Initially, only nitrogen abundances were quantitatively investigated (e.g. Hunter *et al.* 2009), finding both N-rich slow rotators and non-enriched rapid rotators, which apparently challenged stellar evolution models. Soon after it became clear that the consideration of all three elements involved in the CNO cycle has its benefits (Przybilla *et al.* 2010), with the observations following a tight path in the N/C vs. N/O diagram. This diagram shows little dependence on the initial stellar masses, rotation velocities, and nature of the mixing processes, thus this plot constitutes an ideal quality test for observational results (Maeder *et al.* 2014). Abundances provide crucial observational constraints to chemical mixing and angular transport via meridional circulation and shear instabilities

https://doi.org/10.1017/S1743921326106000 Published online by Cambridge University Press

in rotating single star models, and via mass overflow in the course of binary evolution. Important in this context is also the treatment of the transport as a diffusive or (correctly) as an advecto-diffusive process. Nevertheless, relatively few investigations use the potential of complete CNO analyses (e.g. Nieva & Przybilla 2012; Martins *et al.* 2015a,b, 2024; Cazorla *et al.* 2017; Weßmayer *et al.* 2022; Pavlovski *et al.* 2023; Aschenbrenner *et al.* 2023). Boron abundances from analysis of the B III UV resonance lines as constraints to rotational mixing in particular early in the evolution on the MS have come to the attention again recently (e.g. Proffitt *et al.* 2024; Jin *et al.* 2024, and references therein). Models apparently need to account for the magnetic Tayler instability in radiative zones in addition to meridional currents to explain the observations quantitatively, in agreement with additional constraints on angular-momentum transport from asteroseismology (Asatiani *et al.* 2025).

## 3. Quantitative analyses: observational, data reduction and modelling bias

Quantitative analyses of massive stars pose many challenges. These may be observational; in particular, the reduction of Echelle spectra faces the issue of a reliable normalisation of the broad hydrogen lines – often the width of the wings is underestimated, leading to an underestimation of gravity. Comparison with lower-resolution long-slit spectra may be helpful. High-resolution spectroscopy at high-S/N can help to detect minuscule signatures of second light in a spectrum and therefore binarity, even in the absence of time-series spectroscopy. Correct consideration of a second continuum even for a light contribution of a few percent is necessary to minimise systematic errors (see e.g. Aschenbrenner & Przybilla 2024). A similar situation may arise for fast-rotating Be stars, where the decretion disc contributes the second light. Fast rotation poses in general complications, because of the geometric deformation of the star and the resulting gravity darkening (for a discussion of the effects on the quantitative analysis see e.g. Cazorla *et al.* 2017), and the necessity to include all spectral lines because of the strong line blending. A non-homogeneous surface due to non-radial pulsations or due to magnetic spots offers both opportunities to obtain further information (e.g. via time-series spectroscopy for asteroseismology) and complications for analysis (e.g. González *et al.* 2019). In particular, atomic diffusion in very stable atmospheres leads to chemical peculiarities, but with the exception of He-strong stars (e.g. Przybilla *et al.* 2016, 2021), these are fortunately restricted to later spectral types on the MS than to those covered by massive stars. Finally, modelling bias may also arise from the choice of atomic data employed in the model atoms for the non-LTE calculations. The main sources of errors are approximation formulae that are often employed for the calculation of collisional rates; more accurate and precise *ab-initio* data should be preferred, as they are typically available nowadays.

## 4. Hybrid non-LTE analyses

Massive star analyses rely currently for the most part on three hydrodynamic non-LTE line-blanketed model atmosphere codes accounting for spherical geometry, CMFGEN (Hillier & Miller 1998), PoWR (Gräfener *et al.* 2002; Hamann & Gräfener 2003) and FASTWIND (Puls *et al.* 2005, 2020), with many tests undertaken that show overall good consistency of the modelling results (they are complemented by their hydrostatic counterpart in plane-parallel geometry, TLUSTY, Hubeny 1988). While the codes are successfully employed for deriving stellar parameters, the determination of chemical abundances has in most studies been restricted to helium, silicon and nitrogen, and sometimes in addition included also carbon and oxygen. These restrictions originate in the long run-times per

https://doi.org/10.1017/S1743921326106000 Published online by Cambridge University Press

**Table 1.** Non-LTE model atoms and cosmic standard abundance data.

| Element/Ion | Terms | Transitions | Ref. | OB stars log (X/H)+12 | Sun log (X/H)+12 | Δ (OB – Sun) dex |
|---|---|---|---|---|---|---|
| C II/III/IV | 68/70/53 | 425/373/319 | [1] | 8.33±0.04 | 8.46±0.04 | −0.13 |
| N I/II/III/IV | 89/77/47+3/84+6 | 668/462/410/1123 | [2] | 7.79±0.04 | 7.83±0.07 | −0.04 |
| O I/II/III | 51/177+2/132+2 | 243/2560/1515 | [3] | 8.76±0.05 | 8.69±0.04 | 0.07 |
| Ne I/II | 153/78 | 952/992 | [4] | 8.09±0.05 | 8.06±0.05 | 0.03 |
| Mg II | 37 | 236 | [5] | 7.56±0.05 | 7.55±0.03 | 0.01 |
| Al II/III | 54+6/46+1 | 378/272 | [6] | 6.30±0.07* | 6.43±0.03 | −0.13 |
| Si II/III/IV | 52+3/68+4/33+2 | 357/572/242 | [7] | 7.50±0.05 | 7.51±0.03 | −0.01 |
| P II/III/IV | 45/25/23 | 358/81/61 | [8] | 5.36±0.14 | 5.41±0.03 | −0.05 |
| S II/III | 78/21 | 302/34 | [9] | 7.14±0.06* | 7.12±0.03 | 0.02 |
| Ar I/II | 23/56 | 49/596 | [10] | 6.57±0.05* | 6.38±0.10 | 0.19 |
| Fe II/III/IV | 265/60+46/65+70 | 2887/2446/2094 | [11] | 7.52±0.03 | 7.46±0.04 | 0.06 |

The number of superlevels is marked by a preceding '+'; photospheric abundances: Asplund *et al.* (2021); * preliminary values. References: [1] Nieva & Przybilla (2006, 2008); [2] Przybilla & Butler (2001), Przybilla & Aschenbrenner (in prep.); [3] Przybilla *et al.* (2000), Aschenbrenner *et al.* (2023); [4] Morel & Butler (2008); [5] Przybilla *et al.* (2001a); [6] Przybilla (in prep.); [7] Przybilla & Butler (in prep.); [8] Aschenbrenner *et al.* (2025); [9] Vrancken *et al.* (1996), updated; [10] Keiler *et al.* (in prep); [11] Becker (1998), Morel *et al.* (2006).

model (1+ CPU-days, with the exception of FASTWIND) and the availability of detailed model atoms.

An alternative efficient (∼2 CPU-hours) methodology for analysing the spectra of massive blue stars with weak winds is based on a hybrid non-LTE approach (e.g. Przybilla *et al.* 2006; Nieva & Przybilla 2007; Weßmayer *et al.* 2022; Aschenbrenner *et al.* 2023), that is, non-LTE spectral synthesis is performed on LTE line-blanketed model atmospheres. Kurucz's ATLAS9 and ATLAS12 codes (Kurucz 1993, 2005) are used, which assume plane-parallel geometry, hydrostatic, radiative, and local thermodynamic equilibrium, stationarity, and chemical homogeneity. ATLAS12 allows for the effects of turbulent pressure on atmospheric stratification to be considered. Subsequently, non-LTE computations are performed with DETAIL (solving the coupled radiative transfer and rate equations) and SURFACE (calculating the formal solution based on non-LTE level populations and using refined line-broadening data) as introduced by Giddings (1981) and Butler & Giddings (1985). Both codes have been updated and extended in capability over the past 40 years, such as by introducing an accelerated lambda iteration scheme, level dissolution, and state-of-the-art Stark-broadening tables for H I and He I/II.

A strength of the hybrid non-LTE approach is that highly detailed model atoms can be implemented, beyond hydrogen (Przybilla & Butler 2004) and helium (Przybilla 2005). An overview of the available model atoms for analysis of metals in OB stars in the hybrid approach is given in Table 1, where the element/ion combinations are listed, the number of energy terms and the number of radiative bound-bound transitions considered in the calculations. The model atoms typically also account for *ab-initio* data for photoionisation processes, and for a large number of electron-impact excitation data for a realistic description of also the local processes. Almost the entire optical spectra of OB stars can be reliably reproduced with these models.

Three codes are employed for spectral analyses, SPAS (Hirsch 2009), a more advanced semi-automated $\chi^2$-minimisation routine as described by Irrgang *et al.* (2014), and our most sophisticated code implemented so far, SATURN (Aschenbrenner & Przybilla, in prep.), which uses neural networks to emulate spectra of single and multi-star systems with arbitrary atmospheric parameters and chemical composition, and which offers a Markov-Chain Monte Carlo algorithm to derive stellar parameters and chemical abundances, and to constrain uncertainties. In all cases, synthetic spectra are used to fit multiple Stark-broadened hydrogen lines and multiple ionisation equilibria to derive the effective temperature $T_{\rm eff}$ and surface gravity $\log g$. Verification of $T_{\rm eff}$ can be achieved by

https://doi.org/10.1017/S1743921326106000 Published online by Cambridge University Press

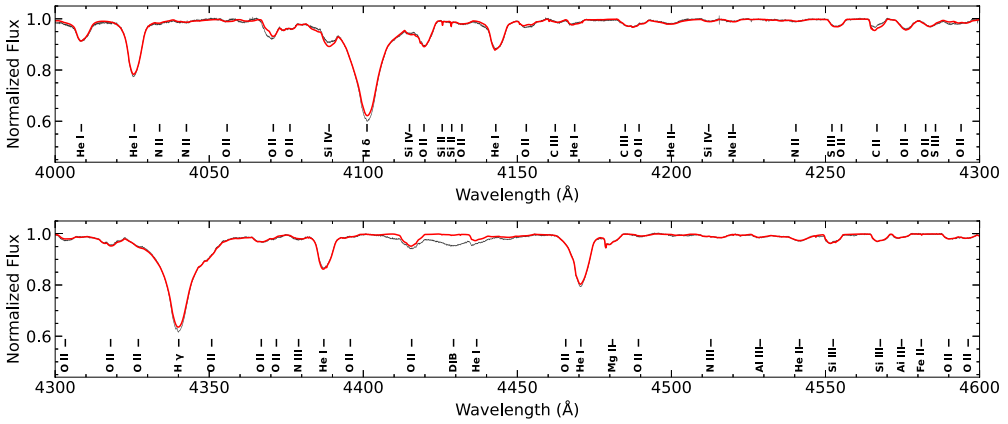



**Figure 1.** Example of a model fit (red line) to an observed optical high-resolution spectrum (black) of a multiple star, the quadruple system HD 37061, exciting star of M 43 in Orion. Only the diffuse interstellar band at 4428 Å is unaccounted for by the model. Adopted from Aschenbrenner & Przybilla (2024).

fitting the spectral energy distribution (SED, which also provides information on interstellar reddening) and of gravity by a comparison of spectroscopic distances and those derived from parallaxes measured by the Gaia mission. The microturbulent velocity $\xi$ is constrained by requiring elemental abundances to be independent of strength of the spectral lines. Abundances are determined by line-profile fits to spectral lines, which requires the (projected) rotational velocity $v \sin i$ and (radial-tangential) macroturbulent velocity $\zeta$ to be constrained at the same time. Subsequently, fundamental stellar parameters, (evolutionary) mass $M$, radius $R$ and luminosity $L$ can also be determined, requiring stellar evolution models to be considered; see, e.g. Nieva & Przybilla (2014). Alternatively, with the extinction constrained from the SED fit and the Gaia distance, one can derive the luminosity, and from this the radius (knowing $T_{\rm eff}$), and finally, using $\log g$, the (spectroscopic) mass.

An example of the fit quality of a hybrid non-LTE model to an observed spectrum of a multiple star is shown in Fig. 1, the quadruple star system HD 37061, which excites the spherical H II region Messier 43 close to the Orion nebula. The analysis (Aschenbrenner & Przybilla 2024) recovers abundances close to the cosmic standard abundances (see below). More examples, in particular of benchmark eclipsing binary systems, are discussed by Aschenbrenner & Przybilla (in prep.). The reliable reproduction of the observations is due to detailed model atoms and allows $T_{\rm eff}$, $\log g$ and elemental abundances to be determined with uncertainties of typically 1-2% and 0.05-0.10 dex ($1\sigma$ standard deviations) for the latter two, and absolute systematic uncertainties in abundances of ∼0.1 dex (e.g. Przybilla *et al.* 2000, 2001a,b).

## 5. Observational constraints on massive star evolution from hybrid non-LTE analyses

Most of the stellar evolution tracks for Galactic massive stars employ a solar abundance mix of metallicity $Z = 0.014$ (Asplund *et al.* 2009) as initial chemical composition input. This is because the most comprehensive information on chemical composition is available for the Sun (see Table 1 for photospheric abundances, the bulk abundances are about 0.04 dex higher), and it appears to reflect the elemental abundances in the solar neighbourhood rather well. On the other hand, it is not clear why a 4.6 Gyr old star should be chemically representative for the young massive star population – ever

https://doi.org/10.1017/S1743921326106000 Published online by Cambridge University Press

ongoing nucleosynthesis in the Milky Way should have increased the metallicity at the present Sun's galactocentric radius over that time, depending on element, like 0.04 dex for oxygen to 0.14 dex for iron (Chiappini *et al.* 2003).

Using hybrid non-LTE analyses, Przybilla *et al.* (2008), Nieva & Simón-Díaz (2011) and in particular Nieva & Przybilla (2012) studied a sample of slowly-rotating early B-type stars within a distance of ∼500 pc of the Sun and found chemical homogeneity. Data of the resulting cosmic abundance standard (CAS, plus results from later work on these and other OB stars) are summarised in Table 1. The comparison with solar photospheric abundances shows agreement for many elements but disagreement for some, in particular for carbon, aluminium, and argon. This is not in contradiction to Galactic chemical evolution. The data can be interpreted such that the Sun migrated radially in the Galactic disc from its birthplace about 2-3 kpc closer to the Galactic Centre to its current position (Wielen *et al.* 1996; Nieva & Przybilla 2012).

Among the most recent applications of hybrid non-LTE models is the determination of the cosmic present-day abundance of phosphorus (Aschenbrenner *et al.* 2025). Its knowledge is important for reliable use of the typically unsaturated P V resonance lines as mass-loss indicators for hotter stars. The thus derived mass-loss rates are lower than those obtained from other indicators by about an order of magnitude, which was interpreted such that the radiatively-driven massive star winds are clumped (Fullerton *et al.* 2006). The revised mass-loss rates, in turn, have a great impact on stellar evolution models.

The small uncertainties in stellar parameters achievable via thorough hybrid non-LTE analyses enable a very accurate and precise positioning of the stars in the HRD, up to masses of $\sim 30\,M_\odot$ (because of the limitations of the hydrostatic model atmospheres); this applies also to the progeny of OB-type stars like BA-type supergiants (e.g. Przybilla *et al.* 2006; Firnstein & Przybilla 2012). Of particular interest are the thus obtainable observational constraints on rotational mixing in the course of stellar evolution, in the form of the abundances of carbon, nitrogen, and oxygen, indicators of the mixing of CNO-cycled matter from the core to the stellar surface. The analysed stars closely follow the path predicted by stellar evolution models in the N/C versus N/O diagram (Przybilla *et al.* 2010), see Fig. 2, implying also a high quality of the derived stellar parameters (Maeder *et al.* 2014). The supergiants show overall a higher degree of mixing. Three recently analysed objects are highlighted in Fig. 2: the SN1987A progenitor-like Sher 25 with its hourglass-shaped surrounding nebula is one of the objects that shows the highest degree of mixing with nuclear-processed material, probably the result of a merger (for a further discussion see Weßmayer *et al.* 2023). HD93840, an extremely nitrogen-enhanced supergiant runaway star at intermediate galactic latitude with a previous binary mass-exchange history that also has a highly-processed bulk composition, indicating a very advanced stage in its evolution (Weßmayer *et al.* 2024); and $\gamma$ Col, which is a stripped and pulsating ∼4 to $5\,M_\odot$ core of an initially $\sim 12\,M_\odot$ star that just finished central hydrogen fusion (Irrgang *et al.* 2022). It mimics an ordinary early B-type subgiant spectrum, with the exception of near-equilibrium abundances of carbon and nitrogen from CN-cycle burning. The star is undergoing structural re-adjustment after the stripping event. Coming analyses of larger star samples with the hybrid non-LTE approach will provide detailed observational constraints on stellar evolution models, as they will also yield other fascinating outliers.

## 6. Pending issues

The imminent next challenges are indeed analyses of large spectroscopic datasets of thousands of massive stars, as will be provided by the William herschel telescope Enhanced Area Velocity Explorer (WEAVE, Jin *et al.* 2024) or the 4-metre Multi-Object Spectroscopic Telescope (4MOST, de Jong *et al.* 2019). Currently, several

https://doi.org/10.1017/S1743921326106000 Published online by Cambridge University Press

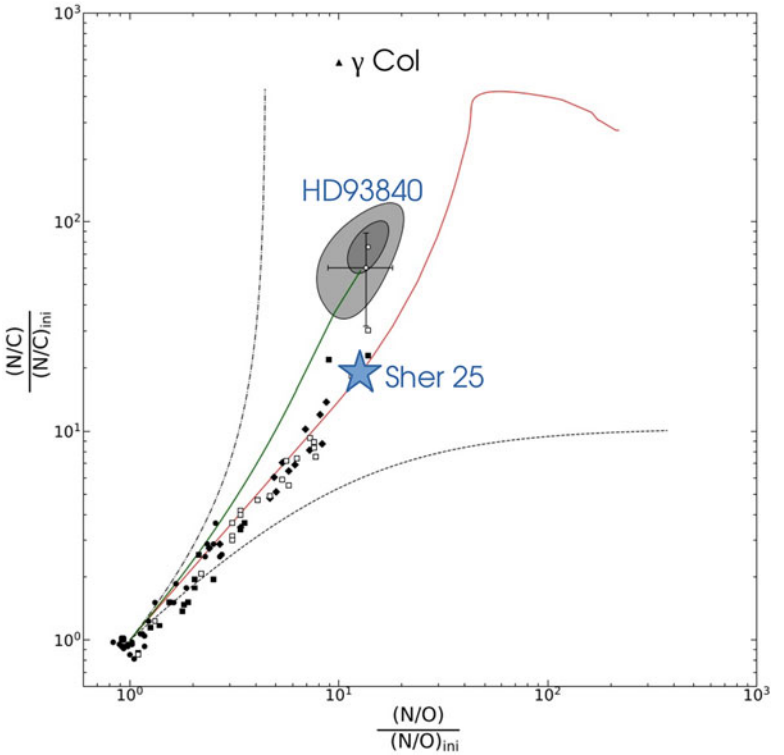



**Figure 2.** N/C ratio vs. N/O ratios for a sample of OB stars (dots, filled boxes) and their progeny, BA-type supergiants (diamonds, open boxes), normalised to initial values. Three of the stars highlighted in the present work are marked. For comparison, the development of the surface CNO abundances is shown for two Geneva evolution tracks. The dashed and dash-dotted lines depict the analytical boundaries for the ON- and CN-cycle, respectively. Based on data described in detail by Weßmayer *et al.* (2024).

(semi)automated approaches exist for the analysis, such as, for example, genetic algorithms (Mokiem *et al.* 2005), grid-based $\chi^2$ minimisation algorithms (e.g. Araya *et al.* 2025), or codes such as MAUI (Urbaneja 2026) that use a Markov chain Monte Carlo algorithm to constrain parameter sets and their uncertainties (for a first application see de Burgos *et al.* 2024, on over 500 targets). First applications on hot stars were undertaken in the framework of the Gaia-ESO survey, on hundreds to thousands of stars (Blomme *et al.* 2022; Morel *et al.* 2022). On a much larger scale, for about 330 000 OBA-type stars, the HOTPAYNE code was employed for LTE modelling of the hot star content of the LAMOST survey (Xiang *et al.* 2022); a necessary extension is the consideration of non-LTE effects. Furthermore, an automated identification of binary and multiple stars with composite spectra also needs to be achieved in order to analyse these objects properly and in an automated fashion. In addition, outliers also need to be reliably identified automatically.

Further work is also required on tight empirical constraints on mass loss rates at all evolutionary stages of massive stars (including the RSG stage, where mass loss is supposed to be most efficient); this will have a noticeable effect on the reliability of stellar evolution models. Finally, – and this still requires a tremendous effort despite observational surveys such as BOB (Morel *et al.* 2015), BINAMICS (Alecian *et al.* 2015) or MIMES (Wade *et al.* 2016) that were targeted to spectropolarimetrically detect surface magnetic fields in massive stars –, additional input is required to derive observational

https://doi.org/10.1017/S1743921326106000 Published online by Cambridge University Press

constraints that will allow the generation and the impact of magnetic fields on massive star evolution to be quantified.

## References


Alecian, E., Neiner, C., Wade, G. A., *et al.* 2015, *Proc. IAU Symp.*, 307, 330
Araya, I., Curé, M., Machuca, N., *et al.* 2025, *A&A*, 704, A77
Asatiani, L., Eggenberger, P., Marchand, M., *et al.* 2025, *A&A*, 699, L8
Aschenbrenner, P., Butler, K. & Przybilla, N. 2025, *A&A*, 698, A164
Aschenbrenner, P. & Przybilla, N. 2024, *A&A*, 691, A361
Aschenbrenner, P., Przybilla, N. & Butler, K. 2023, *A&A*, 671, A36
Asplund, M., Amarsi, A. M. & Grevesse, N. 2021, *A&A*, 653, A141
Asplund, M., Grevesse, N., Sauval, A. J. & Scott, P. 2009, *ARA&A*, 47, 481
Becker, S. R. 1998, *ASP Conf. Ser.*, 131, 137
Blomme, R., Daflon, S., Gebran, M., *et al.* 2022, *A&A*, 661, A120
Brott, I., de Mink, S. E., Cantiello, M., *et al.* 2011, *A&A*, 530, A115
Butler, K. & Giddings, J. R. 1985, *Newsletter of Analysis of Astronomical Spectra*, No. 9 (Univ. London)
Cazorla, C., Morel, T., Nazé, Y., *et al.* 2017, *A&A*, 603, A56
Chiappini, C., Romano, D. & Matteucci, F. 2003, *MNRAS*, 339, 63
Chieffi, A. & Limongi, M. 2013, *ApJ*, 764, 21
Chini, R., Hoffmeister, V. H., Nasseri, A., Stahl, O. & Zinnecker, H. 2012, *MNRAS*, 424, 1925
Choi, J., Dotter, A., Conroy, C., *et al.* 2016, *ApJ*, 823, 102
de Burgos, A., Simón-Díaz, S., Urbaneja, M. A. & Puls, J. 2024, *A&A*, 687, A228
de Burgos, A., Simón-Díaz, S., Urbaneja, M. A., *et al.* 2025, *A&A*, 695, A87
de Jong, R. S., *et al.* 2019, *The Messenger*, 175, 3
de Mink, S. E., Langer, N., Izzard, R. G., Sana, H. & de Koter, A. 2013, *ApJ*, 764, 166
Dufton, P. L., Langer, N., Dunstall, P. R., *et al.* 2013, *A&A*, 550, A109
Eggenberger, P., Meynet, G. & Maeder, A. 2022, *A&A*, 386, 576
Ekström, S., Georgy, C., Eggenberger, P. *et al.* 2012, *A&A*, 537, A146
Firnstein, M. & Przybilla, N. 2012, *A&A*, 543, A80
Fullerton, A. W., Massa, D. L. & Prinja, R. K. 2006, *ApJ*, 637, 1025
Georgy, C., Meynet, G., Walder, R., Folini, D. & Maeder, A. 2009, *A&A*, 502, 611
Giddings, J. R. 1981, Ph.D. Thesis (Univ. London)
González, J. F., Briquet, M., Przybilla, N. *et al.* 2019, *A&A*, 626, A94
Gräfener, G., Koesterke, L. & Hamann, W.-R. 2002, *A&A*, 387, 244
Grunhut, J. H., Wade, G. A., Neiner, C., *et al.* 2017, *MNRAS* 465, 2432
Hamann, W.-R. & Gräfener, G. 2003, *A&A*, 410, 993
He, Y., Song, H., Meynet, G., *et al.* 2025, *ApJ*, 994, 77
Hillier, D. J. & Miller, D. L. 1998, *ApJ*, 496, 407
Hirsch, H. A. 2009, Ph.D. Thesis (Univ. Erlangen-Nuremberg)
Hubeny, I. 1988, *Comput. Phys. Commun.*, 52, 103
Hunter, I., Brott, I., Langer, N., *et al.* 2009, A&A, 496, 841
Irrgang, A., Przybilla, N., Heber, U. *et al.* 2014, *A&A*, 565, A63
Irrgang, A., Przybilla, N. & Meynet, G. 2022, *Nat. Astron.*, 6, 1414
Jin, H., Langer, N., Lennon, D. J., *et al.* 2024, *A&A*, 690, A135
Jin, S., Trager, S. C., Dalton, G. B. *et al.* 2024, *MNRAS*, 530, 2688
Keszthelyi, Z., de Koter, A., Götberg, Y., *et al.* 2022, *MNRAS*, 517, 2028
Kurucz, R. L. 1993, CD-ROM No. 13 (Cambridge, Mass.: SAO)
Kurucz, R. L. 2005, *Mem. Soc. Astron. Ital. Suppl.*, 8, 14
Langer, N. & Maeder, A. 1995, *A&A*, 295, 685
Maeder, A., Przybilla, N., Nieva, M. F. *et al.* 2014, *A&A*, 565, A39
Marchant, P. & Bodensteiner, J. 2024, *ARA&A*, 62, 21
Martins, F., Bouret, J.-C., Hillier, D. J., *et al.* 2024, *A&A*, 689, A31
Martins, F., Hervé, A., Bouret, J.-C., *et al.* 2015a, *A&A*, 575, A34


https://doi.org/10.1017/S1743921326106000 Published online by Cambridge University Press

Martins, F. & Palacios, A. 2013, *A&A*, 560, A16
Martins, F., Simón-Díaz, S., Palacios, A., *et al.* 2015b, *A&A*, 578, A109
Meynet, G. & Maeder, A. 2005, *A&A*, 429, 581
Mokiem, M. R., de Koter, A., Puls, J., *et al.* 2005, *A&A*, 441, 711
Morel, T., Blazère, A., Semaan, T., *et al.* 2022, *A&A*, 665, A108
Morel, T., Butler, K., Aerts, C. *et al.* 2006, *A&A*, 457, 651
Morel, T. & Butler K. 2008, *A&A*, 487, 307
Morel, T., Castro, N., Fossati, L., *et al.* 2015, *Proc. IAU Symp.*, 307, 342
Nieva, M. F. & Przybilla, N. 2006, *ApJ*, 639, L39
Nieva, M. F. & Przybilla, N. 2007, *A&A*, 467, 295
Nieva, M. F. & Przybilla, N. 2008, *A&A*, 481, 199
Nieva, M. F. & Przybilla, N. 2012, *A&A*, 539, A143
Nieva, M. F. & Przybilla, N. 2014, *A&A*, 566, A7
Nieva, M. F. & Simón-Díaz, S. 2011, *A&A*, 532, A2
Pavlovski, K., Southworth, J., Tkachenko, A. *et al.* 2023, *A&A*, 671, A139
Proffitt, C. R., Jin, H., Daflon, S. *et al.* 2024, *ApJ*, 968, 1
Przybilla, N. 2005, *A&A*, 443, 293
Przybilla, N. & Butler, K. 2001, *A&A*, 379, 955
Przybilla, N. & Butler, K. 2004, *ApJ*, 609, 1181
Przybilla, N., Butler, K., Becker, S. R. & Kudritzki, R. P. 2001a, *A&A*, 369, 1009
Przybilla, N., Butler, K., Becker, S. R. & Kudritzki, R. P. 2006, *A&A*, 445, 1099
Przybilla, N., Butler, K., Becker, S. R. & Kudritzki, R. P. & Venn, K. A. 2006, *A&A*, 359, 1085
Przybilla, N., Butler, K. & Kudritzki, R. P. 2001b, *A&A*, 379, 936
Przybilla, N., Firnstein, M., Nieva, M. F., *et al.* 2010, *A&A*, 517, A38
Przybilla, N., Fossati, L., Hubrig, S., *et al.* 2016, *A&A*, 587, A7
Przybilla, N., Fossati, L. & Jeffery, C. S. 2021, *A&A*, 654, A119
Przybilla, N., Nieva, M. F. & Butler,K. 2008, *ApJ*, 688, L103
Puls, J., Urbaneja, M. A., Venero, R., *et al.* 2005, *A&A*, 435, 669
Puls, J., Najarro, F., Sundqvist, J. O., *et al.* 2020, *A&A*, 642, A172
Sana, H., de Mink, S. E., de Koter, A., *et al.*2012, *Science*, 337, 444
Schöller, M., Hubrig, S., Fossati, L., *et al.* 2017, *A&A*, 599, A66
Urbaneja, M. A. 2026, *A&A*, in press [arXiv:2601.01491]
Vrancken, M., Butler, K. & Becker, S. R. 1996, *A&A*, 311, 661
Wade, G. A., Neiner, C., Alecian, E., *et al.* 2016, *MNRAS*, 456, 2
Weßmayer, D., Przybilla, N. & Butler, K. 2022, *A&A*, 668, A92
Weßmayer, D., Przybilla, N., Ebenbichler, A., *et al.* 2023, *A&A*, 677, A175
Weßmayer, D., Urbaneja, M. A., Butler, K. & Przybilla, N. 2024, *A&A*, 687, L7
Wielen, R., Fuchs, B. & Dettbarn, C. 1996, *A&A*, 314, 438
Xiang, M. Rix, H. W., Ting, Y. S. *et al.* 2022, *A&A*, 662, A66

https://doi.org/10.1017/S1743921326106000 Published online by Cambridge University Press